RSC Advances

ROYAL SOCIETY OF CHEMISTRY

www.rsc.org/advances

RSC Advances

RSCPublishing

ARTICLE

Continuous Polyacrylonitrile Nanofiber Yarns: Preparation and Dry-drawing Treatment for Carbon Nanofiber Production†

Cite this: DOI: 10.1039/x0xx00000x

Received 00th January 2012,
Accepted 00th January 2012

DOI: 10.1039/x0xx00000x

www.rsc.org/

Zhigang Xie, Haitao Niu, Tong Lin,*

Precursor fibers with diameter on nanometer scales and highly aligned polymer chains in fibers are highly promising to prepare high-performance carbon nanofibers, but are challenging to make. In this study, we for the first time demonstrate that a carbon nanofiber precursor can be prepared by electrospinning of polyacrylonitrile into a nanofiber yarn and by subsequent drawing treatment of the yarn at a dry condition. The yarn showed excellent drawing performance, which can be drawn evenly up to 6 times of its original length without breaking. The drawing treatment improved yarn and fiber uniformity, polymer chain orientation within fibers, and yarn tensile and modules, but decreased yarn and fiber diameter and elongation at break. The drawing temperature and force showed influences on the drawing behavior. The highest strength and modules (362 ± 37 MPa and 9.2 ± 1.4 GPa, respectively) were found on the yarn drawn by 5 times its length, which increased by 800% and 1800% when compared to the as-spun yarn. Through un-optimized stabilization and carbonization treatments, we further demonstrate that the carbonized nanofiber yarn shows comparable tensile properties to the commercial carbon fibers. Electrospun nanofiber yarns may form next generation precursors for making high performance carbon fibers.

Introduction

High-performance carbon fibers (HPCFs) are featured by high tensile strength (2 ~ 7 GPa) and high modulus (228 ~ 392 GPa) but very light weight [1]. They are widely used as a structural material where a high strength-to-weight ratio is required, such as aerospace [2, 3], wind turbine [4] and automobile [5]. Recent increase in the demand for HPCFs has led to active development of carbon fiber production technology.

HPCFs can be derived from polyacrylonitrile (PAN) or pitch. Although pitch derived carbon fibers exhibit very high modulus, they are more rigid and have low strain level, typically below 2% [6]. A significant proportion of HPCFs is made from PAN [6, 7]. To form HPCFs, PAN precursor fibers are prepared normally by a wet spinning technique, and then subjected to a series of treatments, including drawing, stabilization and carbonization. Uniaxial drawing makes polymer chains highly orientated within the precursor fibers, minimizing the defects per unit length in the precursor fiber and meanwhile reducing fiber diameter from tens of to a few micrometers. The drawn fibers are then stabilized (also known as oxidized) by heating at a temperature around 250 °C ~ 500 °C in air to turn into infusible [8, 9]. Further carbonizing at higher temperatures (e.g. 600 °C ~ 1600 °C) in an inert environment results in HPCFs [10].

Despite T-1000 carbon fibers with a tensile strength as high as 7.07 GPa have been available commercially [7], the ultimate tensile strength of HPCFs does not exceed 25% of the theoretically estimated value [6, 8]. The lower tensile strength than the theoretical prediction originates primarily from structural defects generated in the carbon fiber production process [11, 12]. For example, fiber coagulation and associated solvent diffusion between polymer and coagulant during wet spinning may cause phase separation and formation of voids, cracks, or cavities within fibers [11, 13, 14]. Core-sheath structure may occur when the inner core of fiber is oxidized incompletely during the stabilization step, and carbon fibers prepared from such a core-shell structure have poor mechanical properties due to burning off the core in the carbonization process [15, 16].

Reducing fiber diameter is an effective solution to minimize structure defects thus improve its mechanical properties. It also facilitates the stabilization of precursor fibers, thus diminishing the formation of core-shell structures. A good example is T-1000 carbon fibers, the diameter (5.0 μm) of which is just 2.7 micron less than T-300 (7.7 μm); however, the tensile strength (7.07 GPa) is 2.97 GPa greater (see the tensile property of other HPCFs in Fig. S1) [17]. It is expected that carbon nanofibers (CNFs) deliver tremendous improvement in the mechanical properties because of the small diameter, which are several orders of magnitude smaller than existing carbon fibers [16]. Precursor fibers prepared without involving a coagulation process avoids solvent diffusion and associated defect formation.

Electrostatic spinning, also known as electrospinning, offers a unique opportunity to prepare ultrafine precursor fibers without involving any coagulation process. It involves drawing a

polymer solution under a strong electric field to form dry filaments. Without coagulation, fibers are formed by fast evaporation of solvent from a polymer solution jet during electrospinning. Electrospinning has been used to prepare PAN fibers, which have a diameter typically about hundreds of nanometer [18]. Several papers reported the production of carbon fibers from electrospun PAN nanofibers [19, 20]. A single CNF was reported to have a bending modulus of 63 GPa and a fracture strength of 0.64 GPa with a failure probability of 63% [21]. Separately, the tensile strength and elastic modulus of single CNFs were reported, being 3.5 ± 0.6 GPa and 172 ± 40 GPa, respectively [22]. Short CNF bundles prepared from electrospun nanofiber mats showed a tensile strength of 986 MPa [23] and a modulus of 58 GPa [24]. The lower tensile strength than conventional carbon fibers was attributed to un-optimized processing condition [20, 24].

With the conventional technique to produce carbon fibers, drawing of precursor fibers before stabilization plays a key role in improving polymer molecular orientation and crystallinity, as well as lowering defects within fibers [25-28], which determine the final mechanical properties [8]. PAN is a semi-crystal polymer with a glass transition temperature (Tg) in the range of 72 °C ~ 150 °C [29-31]. Above Tg, PAN fibers become plastic and can be drawn to a large ratio. The conventional PAN precursor fibers are drawn in either an aqueous solution or a steam environment at an elevated temperature (e.g. 40 °C ~ 170 °C) [32-34]. However, drawing treatment of electrospun nanofibers for carbon fiber production has little been reported in the research literature [26].

One of the difficulties in drawing treatment of electrospun nanofibers comes from the randomly-orientated fibrous structure. In most of cases, nanofibers are electrospun into a nonwoven fiber mat, and it is difficult to stretch such a thin, low strength, two-dimensional fiber web uniformly. Electrospinning nanofibers into yarns, i.e. continuous nanofiber bundles with an interlocked fibrous structure, offers a promising solution to drawing nanofibers effectively and continuously.

Considerable efforts have been devoted to directly electrospin nanofiber yarns over recent years. Nanofiber yarns have been electrospun using liquid bath [35-38], solid surface collector [39-41] or rotary funnel [42, 43]. In our previous study, we have developed an effective technique to electrospin highly-twisted continuous nanofiber yarns [43], Using poly(vinylidene fluoride-co-hexafluoropropene) as a model polymer, we examined the effect of working parameters on yarn dimension, twist structure and tensile property. The yarns showed better mechanical property than nonwoven mats.

Herein, we report the preparation of continuous PAN nanofiber yarns and effect of a post-electrospinning drawing treatment on fiber/yarn dimension and tensile property. We found that PAN nanofiber yarns can be drawn up to 6 times its original length under a hot, dry condition without using an aqueous solution and steam. Drawing treatment reduced fiber diameter, but considerably improved fiber uniformity and alignment. The yarn tensile strength and modulus can be increased by 800% and 1800%, respectively, after drawing treatment. We further demonstrated that carbon nanofibers made of the post-drawn PAN nanofiber yarn has a tensile strength of 1.12 ± 0.18 GPa. To the best of our knowledge, it is the first report of drawing treatment of PAN nanofiber yarns and the effect on fiber mechanical properties.

Experimental

Materials

Polyacrylonitrile (PAN, Mw 150,000 g/mol) and N, N′-dimethylformide (DMF) from Sigma-Aldrich were used as received. PAN solution (10 wt%) was prepared by dissolving PAN in DMF at 80 °C.

Electrospinning nanofiber yarns

A purpose-made electrospinning system was used for producing PAN nanofiber yarns. A back metal electrode (diameter 8 cm, thickness 2 mm) was added to each electrospinning nozzle, and two power supplies, one having a positive electrode (ES30P, Gamma High Voltage Research) and another negative (ES30N, Gamma High Voltage Research), were used to drive the two electrospinning nozzles separately. Two electrospinning nozzles were placed in 60 degrees to the funnel axis on opposite side of the funnel. Nozzle to funnel distance was set at 25 cm. To prepare a nanofiber yarn, both positively and negatively charged nanofibers were electrospun and deposited to the large end of the funnel to form a thin nanofiber web. The winding rate and funnel rotating speed were set at 0.32m/min and 245 rpm, respectively. The nanofiber web was then initially manually deformed to be a 3D cone, a nanofiber yarn can be stretched from the apex of the cone. The rotating speed of funnel was adjusted so that a fibrous cone is formed stably on the funnel. A continuous PAN nanofiber yarn can be winded for hours without breaking.

Drawing treatment

Batch yarn drawing was carried out in an oven. 10 pieces of nanofiber yarns (with gauge length 20mm) were firstly with both ends mounted onto opposite sides on a paper frame using double side tapes. The paper frame was then cut on adjacent sides to the yarn mounting edges to release the load to the yarns. Nanofiber yarns were drawn under a constant load (calculated based on optimum value from DMA results) at 140 °C. One edge of the paper frame was fixed at the top grate of the oven and another was applied with the weight load. Drawn by the gravity, the yarn stopped at a pre-set length (drawing ratio). The post drawn nanofiber yarns were then cooled down to room temperature for various characterizations.

Stabilization and carbonization

The stabilization treatment of nanofiber yarns was carried out under constant load (0.5 cN) at 250 °C for 4 hours in an oven. Yarn was clamped at one end and hanged on top grate of the oven, and another end was clamped and was applied with the load. The carbonization was conducted in a tube furnace at 800 °C for 1 hour without tension. Nitrogen was purged initially and maintained a constant flow rate through the carbonization process.

Characterizations

The morphology of nanofibers and yarns was observed under a scanning electron microscope (Jeol, Neoscope SEM). Fiber and yarn diameters were measured based on SEM images using an image analysis software (ImagePro+4.5, Media Cybernetics Co.). Glass transition temperature was measured using the Q800 Dynamic Mechanical Analyzer (DMA) (TA instruments) under a vibration frequency of 10 Hz and a heating rate of 5 °C/min from 40 °C to 200 °C. The thermal mechanical properties were examined in three methods: 1) constant displacement (400 μm/min) at holding temperatures and 2) constant force at elevating temperature from 40 °C to 300 °C (heating rate, 1

°C/min). The molecular orientation in nanofiber was characterized using Fourier transform infrared spectroscope (FTIR) (Brucker Vertex 70) at 64 scan rate. A polarized IR lens was used to obtain polarized IR beam. Tensile properties were examined using FAVIMAT single fiber tester (Textechno). Yarn samples were tested with the gauge length of 20 mm and the crosshead speed of 2 mm/min. The cross-sectional area of nanofiber yarns was calculated from denier of the yarns and density of PAN [44]. Young's modulus and strain at break were average value of 5 repeated measurements.

Fig. 1a & b illustrates the apparatus for electrospinning of PAN nanofiber yarns. Oppositely charged nanofibers were prepared from two electrospinning spinnerets, and a fibrous cone was then formed on a metal funnel collector. A fiber bundle was drawn continuously from the apex of the fibrous cone, and twists were inserted in the meanwhile through the rotation of the funnel collector. PAN nanofiber yarn was collected with a winder. Fig. 1c shows a fibrous cone formed on the funnel collector, and nanofiber yarn collected on a spool is shown in Fig. 1d.

Results and Discussion

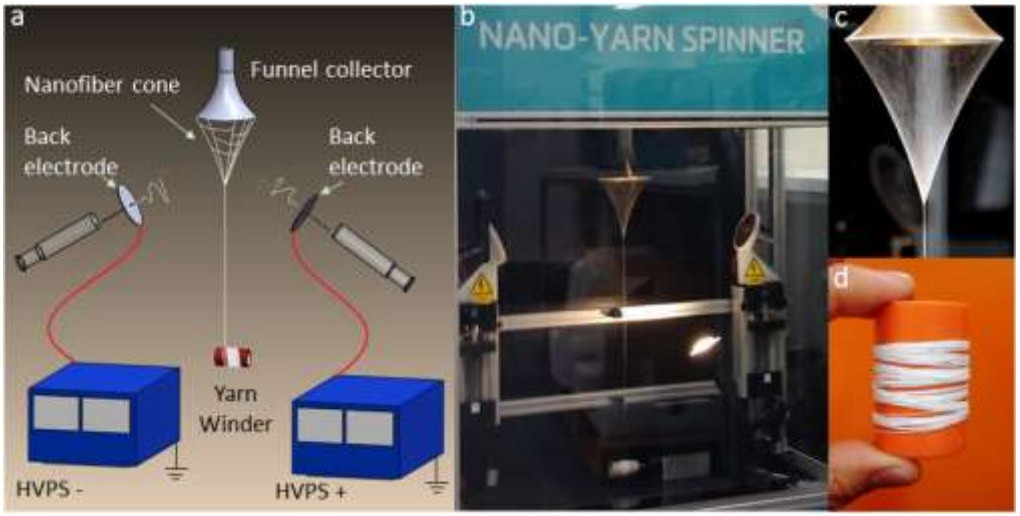

Fig. 1 a) Schematic illustration of a yarn electrospinning setup, b) photo of the fibrous cone, c) nanofiber yarn collected on a spool, d) photo of the actual setup and yarn electrospinning process.

Fig. 2a shows the typical morphology of nanofiber yarns prepared. A good proportion of fibers aligned in an angle along the yarn axis. Fluffy fiber coils and curled fibers were also found on yarn surface. The yarn had a diameter of 279 ± 30 μm and the PAN fibers were 812 ± 312 nm in diameter.

RSC Advances

RSCPublishing

ARTICLE

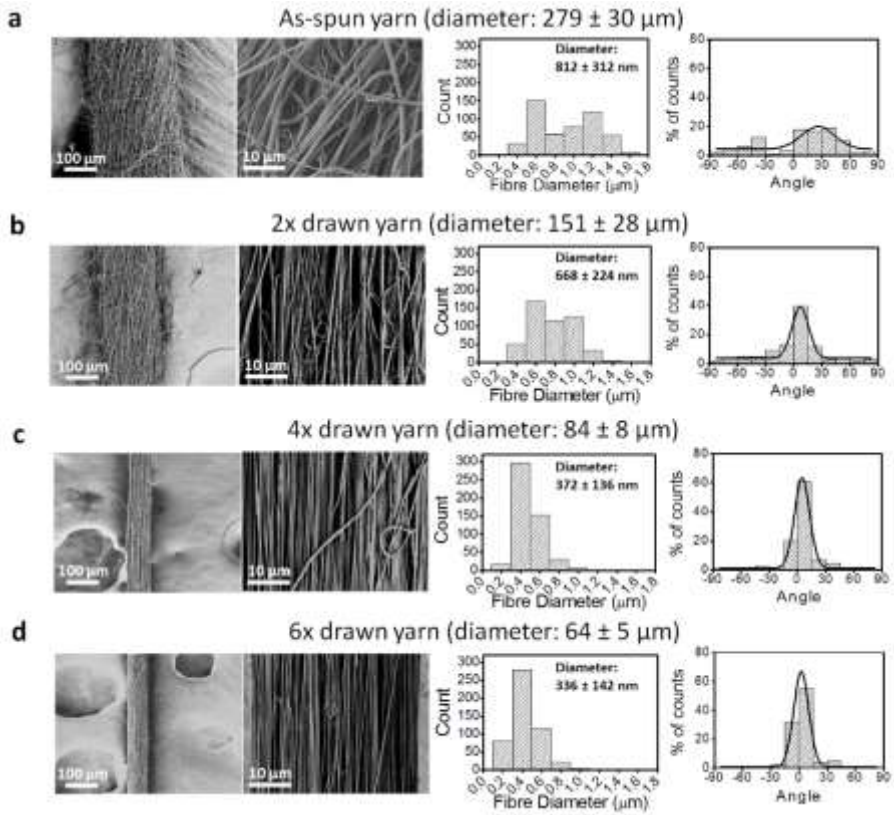

Fig. 2 SEM images of nanofiber yarns and fiber, histogram of fiber diameter distributions and angles of nanofibers along the yarn axis.

It was noted that the twist level in the as-spun nanofiber yarn was lower in comparison to our previously reported PVDF-HFP nanofiber yarns [43], although the setup used for making the two nanofiber yarns was very similar. The different twist feature was attributed to the difference in yarn electrospinning conditions. In the present work, PAN nanofiber yarn was prepared at a low funnel speed (245 rpm). Increasing the funnel speed can increase the twist level. However, PAN nanofiber yarn was hard to be prepared at higher funnel speed because PAN nanofibers are brittle, and nanofiber yarn produced was easy to break at higher funnel speed.

At room temperature, PAN fibers often have a low strain level, while the chain mobility within the fiber increases considerably at a temperature above the Tg. However, when temperature is higher than 250 °C, degradation takes place [45]. In our study, the temperature for drawing PAN fiber yarn was chosen above the Tg but lower than the degradation temperature. Before drawing treatment, the Tg of PAN nanofiber yarn was examined using DMA and DSC. Fig. 3a shows the storage modulus (E′) ~ temperature curve. The maximum storage modulus indicated that Tg was 105 °C (see DSC result in Fig. S2), which was in consistent with the previous report [46].

RSC Advances

RSCPublishing

ARTICLE

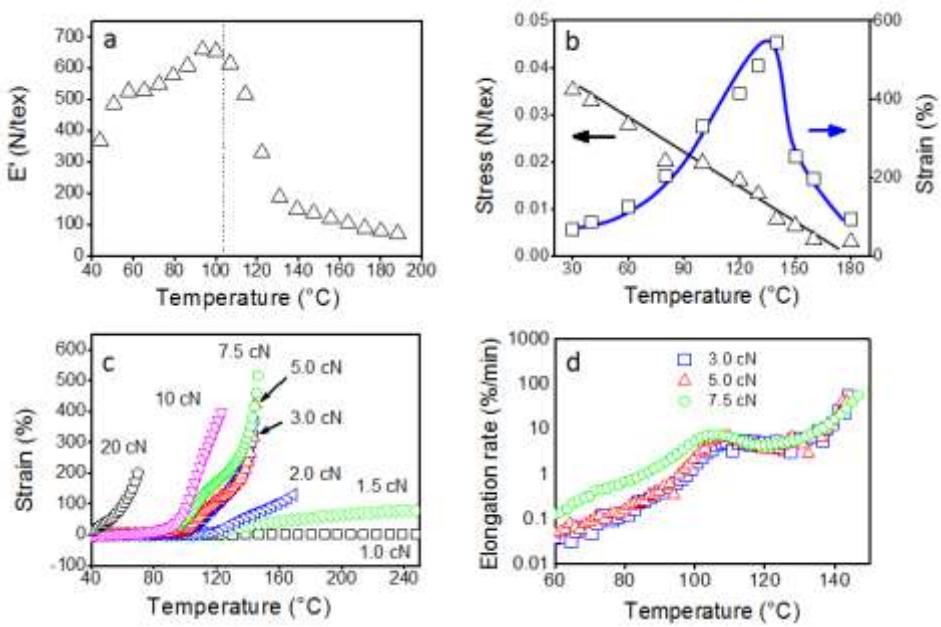

Fig. 3 a) Storage modulus (E') ~ temperature curve of PAN nanofiber yarns (heating rate 5 °C/min, frequency vibration 10 Hz), b) the strain and breaking stress with temperature (yarn was drawn under constant displacement 400 μm/min), c) Strain ~ temperature curves of nanofiber yarns drawn under different forces, d) Strain rate ~ temperature curves of nanofiber yarns drawn with 3.0 cN, 5.0 cN and 7.5 cN force. (Heating rate for c and d is 1 °C/min).

Fig. 3b shows the effect of drawing temperature on the tensile strength and strain at break of nanofiber yarn. At 30 °C, the yarn can only be drawn up to a strain of 69% before breaking. The strain increased gradually with increasing the temperature when the temperature was below 90 °C, while a larger increase of the strain at break with increasing the temperature took place in the temperature range from the Tg to 140 °C. At a higher temperature, the strain then reduced rapidly. At Tg, the strain was about 330%, while the yarn showed the highest strain value (543%) at 140 °C. The tensile strength decreased linearly with increasing drawing temperature.

Fig. 3c shows the strain change of a nanofiber yarn at a constant tension when it is heated up at a constant rate (1 °C/min). The tension force affected the maximum temperature that the yarn can be heated up. At 2.0 cN, the nanofiber yarn can be drawn continuously until the temperature reached 250 °C. Higher drawing force between 2.0 cN and 10.0 cN led to reduce in the upper temperature limit, to 180 °C. Further increasing the drawing force led to a considerable reduction of the temperature range. The tension force also affected the maximum strain. A low tension force led to a small strain value. With increasing the force, the maximum strain increased. At 7.5 cN, the strain reached the maximum value (530%), suggesting the nanofiber yarn can be drawn at the largest drawing ratio.

A two-stage strain response with temperature increase was observed when the yarn was drawn at a force of 3.0 cN ~ 7.5 cN. The 1st stage took place between Tg and 130 °C, and the 2nd started at around 140 °C until the upper temperature limit. The low temperature stage stemmed from the movement of short polymer chain segments under stretching, while higher temperature was required to move longer chain segments. Such a two-stage strain change suggested that elongation rate changed with temperature when the yarn was drawn at a constant force.

Fig. 3d shows elongation rate change during heating a nanofiber yarn at rate 1 °C/min) and a constant tension force. At 3.0 cN, a maximum elongation rate (7 %/min) occurred at around 112 °C, which is in the 1st stage elongation. The elongation rate then reduced gradually to a minimal value (4 %/min) at around 128 °C, and finally increased monotonously (up to 150 %/min) until the yarn broke at 145 °C. At higher tension force, the maximum elongation rate moved to a lower temperature. However, the elongation rate at the upper temperature limit was little affected. This result reflects the competition of molecule movement and chain relaxation under an external tension force. At a small force (e.g. lower than 3.0 cN), polymer chains cannot be drawn to move unless the temperature is above the Tg. The gentle elongation allows a sufficient chain movement with temperature increase. Increasing the force facilitates the chain movement. However, the temperature upper limit is not affected by variation of drawing force much. In this case, the chain movement is not accelerated unless the force is high enough. When the tension force is above 10.0 cN, the tension is so strong that the yarn breaks before it is fully stretched. A force (e.g. 3.0 cN ~ 7.5 cN) between the two extreme states leads to an initially

accelerated stretching at a relatively low temperature followed by further fully stretching a higher temperature, showing a two-stage change in elongation rate. Drawing under a suitable force at a temperature close to 140 °C is effective to elongate the PAN nanofiber yarn to a high strain value.

Fig. 2 also shows yarn morphology after drawing treatment. Here, drawing ratio (i.e. ratio between the elongated and the initial yarn lengths) was employed to represent the elongation length. At a higher drawing ratio, the yarns became more compact and curled fibers became straightened. Yarn and fiber diameters were both decreased after drawing treatment. When the drawing ratio was 3 times, the average yarn and fiber diameters reduced to 91 ± 7 μm and 408 ± 141 nm, respectively. Higher drawing ratio, such as 6 times, further reduced the yarn and fiber diameters to 64 ± 5 μm and 336 ± 142 nm.

In addition to the decrease in diameter, diameter distribution became narrower after drawing treatment (Fig. 2). Without stretching, PAN fibers within the as-spun yarn had a wide diameter distribution, in a range between 300 nm ~ 1.6 μm. After drawing treatment (drawing ratio, 6 times), the fiber diameter range changed to 100 nm ~ 900 nm. Higher drawing ratio did not further narrow the fiber diameter range much, except that the average fiber diameter decreased.

After drawing treatment, the fiber alignment angle along the yarn axis (also referred to as alignment angle) decreased (see Fig. 2). For non-drawn yarn, the fibers had an alignment angle of 0° ~ 60°. After drawing for 2 times of the yarn length, the alignment angle reduced significantly to 30°. Higher drawing ratio led to high alignment of fibers with an alignment angle as small as 15°. The effect of drawing treatment on polymer chain orientation within PAN fibers was also examined by measuring the nitrile group vibration band (C≡N, peak wavenumber 2244 cm-1) in polarized FTIR. Chain-orientation factor (f) was calculated according to equations [47, 48]:

$$D = \frac{A_{\parallel}}{A^{\perp}} \quad (1)$$

$$f = \frac{(D-1)(D_0+2)}{(D_0-1)(D+2)} \quad (2)$$

Where D is the dichroic ratio of C≡N vibration peak intensity (A) under parallel (∥) and perpendicular (⊥) IR beams. D_0 is the dichroic ratio of the polymer with perfect orientation [49]. Fig. 4a shows the D at different beam angle. Drawing treatment increased the D value, indicating that the drawing process facilitated the PAN molecule orientates along the fiber length. The effect of drawing ratio on chain orientation is shown in Fig. 4b. The f value increased with increasing the drawing ratio. The highest f, 0.63, was found on the nanofiber yarn drawn to 6 times of its length. The f at 0 and 1 respectively indicates random and perfectly orientated states.

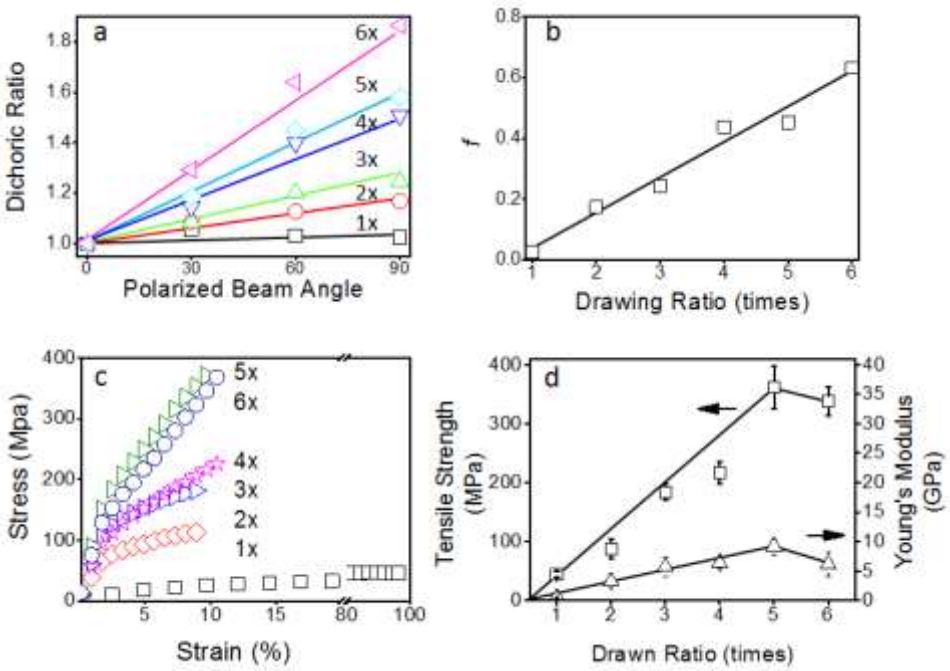

Fig. 4 a) Dichroic ratio at different beam angles, b) effect of drawing ratio on orientation factor, c) strain ~ stress curves of nanofiber yarns under different drawing ratios, d) effect of drawing ratio on yarn tensile strength and Young's modulus.

Fig. 4c & d show the stress ~ strain curves and effect of drawing ratio on the tensile strength and Young's modulus of nanofiber yarns. With increasing the drawing ratio, both the tensile strength and the Young's modulus increased until the drawing ratio reached 5 times. The 5-times drawn yarns had a tensile strength and a Young's modulus of 362 ± 37 MPa and 9.2 ± 1.4 GPa, respectively, which were more than 800% and 1800% of as-spun yarns. In addition, the drawing treatment significantly decreased the strain level. This was attributed to the increased nanofiber alignment and polymer chain after drawing treatment.

To prove the feasibility of forming carbon nanofibers from nanofiber yarn, a PAN nanofiber yarn after 5 times drawing treatment was subjected to stabilization and carbonization treatments. Fig. 5a shows the SEM images of the carbonized nanofiber yarn, which has similar morphology to the precursor yarn. After carbonation, nanofiber and yarn diameters changed to 44.29 ± 0.09 μm and 190.02 ± 31.79 nm respectively. The

stress-strain curve of the carbon nanofiber yarn showed some elongation and its modulus changed from 3 GPa to 40 GPa when the strain changed 1% to 2.5% (Fig. 5b). The tensile strength was 1.12 ± 0.18 GPa. Such a relatively low tensile strength value was attributed to the un-optimized stabilization/carbonization condition and nanofiber structure. A systematic study will be conducted to make high strength carbon nanofibers based on PAN nanofiber yarns in future.

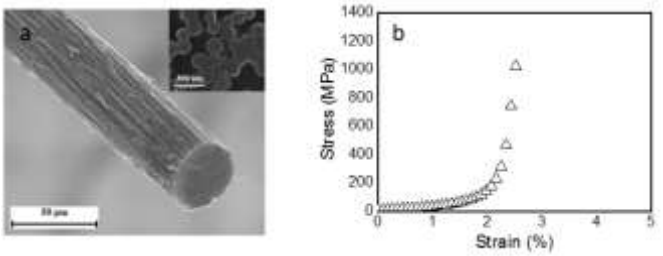

Fig. 5 a) SEM images of PAN nanofiber yarn after stabilization and carbonization treatments (embedded picture shows the cross section of carbon nanofibers, b) stress~ strain curve of resultant carbon nanofiber yarn.

Conclusions

We have demonstrated that a continuous PAN nanofiber yarn can be prepared directly by an electrospinning technique. The yarn shows excellent drawing performance at a dry condition. The drawing treatment improves yarn and fiber uniformity, fiber alignment, polymer chain orientation, and yarn tensile strength, but decreases yarn and fiber diameter and elongation at break. Drawing temperature and force show influences on yarn drawing behavior. The nanofiber yarns after stabilization and carbonization treatments maintain the fibrous morphology, and the carbonized nanofiber yarns show comparable tensile properties to the commercial carbon fibers. Electrospun nanofiber yarns may form a next generation precursor for making high performance carbon fibers.

Notes and references

Institute for Frontier Materials, Deakin University, VIC 3126, Australia; Corresponding author, Tel: +61-(0)3-5227 1225, E-mail address: tong.lin@deakin.edu.au

† Electronic Supplementary Information (ESI) available: The relationship between strain at break and tensile strength of carbon fibers. DSC results of PAN power and nanofiber yarns. See DOI: 10.1039/b000000x/

1. D. D. L. Chung, *Carbon Fiber Composites*, Butterworth-Heinemann, 1994.
2. G. Norris, *Airbus A380: Superjumbo of the 21st Century*, Zenith press, 2005.
3. D. Brosius, in *High-performance Composites*, Gardner business media. inc., 2007.
4. D. A. Griffin and T. D. Ashwill, *Journal of Solar Energy Engineering-Transactions of the Asme*, 2003, **125**, 515-521.
5. G. Savage, *Honda Racing F1*, 2008, **2008**, 1-31.
6. E. Fitzer, *Carbon*, 1989, **27**, 621-645.
7. D. Johnson, *Carbon Fibers Filaments and Composites*, Kluwer Academic Publisher, 1990.
8. P. Morgan, *Carbon Fibers and Their Composites*, TAYLOR & FRANCIS LTD, 2005.
9. Z. Bashir, *Carbon*, 1991, **29**, 1081-1090.
10. M. S. A. Rahaman, A. F. Ismail and A. Mustafa, *Polym. Degrad. Stab.*, 2007, **92**, 1421-1432.
11. J. W. Johnson and D. J. Thorne, *Carbon*, 1969, **7**, 659-661.
12. D. J. Thorne, *Nature*, 1974, **248**, 754-756.
13. S. H. Bahrami, P. Bajaj and K. Sen, *J. Appl. Polym. Sci.*, 2003, **89**, 1825-1837.
14. L. Tan, H. Chen, D. Pan and N. Pan, *J. Appl. Polym. Sci.*, 2008, **110**, 1997-2000.
15. B. F. Jones, *J. Mater. Sci.*, 1971, **6**, 1225-1227.
16. J. Liu, Z. R. Yue and H. Fong, *Small*, 2009, **5**, 536-542.
17. K. Naito, J.-M. Yang, Y. Tanaka and Y. Kagawa, *J. Mater. Sci.*, 2012, **47**, 632-642.
18. J. Chen, H. Ge, H. Liu, G. Li and C. Wang, *Journal of Wuhan University of Technology-Mater. Sci. Ed.*, 2010, **25**, 200-205.
19. S. Y. Gu, J. Ren and Q. L. Wu, *Synth. Met.*, 2005, **155**, 157-161.
20. S. F. Fennessey, Doctoral Doctoral Dissertations, University of Massachusetts, 2006.
21. E. Zussman, X. Chen, W. Ding, L. Calabri, D. A. Dikin, J. P. Quintana and R. S. Ruoff, *Carbon*, 2005, **43**, 2175-2185.
22. S. N. Arshad, M. Naraghi and I. Chasiotis, *Carbon*, 2011, **49**, 1710-1719.
23. S. Moon and R. J. Farris, *Carbon*, 2009, **47**, 2829-2839.
24. Z. P. Zhou, C. L. Lai, L. F. Zhang, Y. Qian, H. Q. Hou, D. H. Reneker and H. Fong, *Polymer*, 2009, **50**, 2999-3006.
25. D. Sawai, Y. Fujii and T. Kanamoto, *Polymer*, 2006, **47**, 4445-4453.
26. C. L. Lai, G. J. Zhong, Z. R. Yue, G. Chen, L. F. Zhang, A. Vakili, Y. Wang, L. Zhu, J. Liu and H. Fong, *Polymer*, 2011, **52**, 519-528.
27. L. J. Tan and A. Wan, *Colloids and Surfaces a-Physicochemical and Engineering Aspects*, 2011, **392**, 350-354.
28. W. Qin, L. Xiaoyi, L. Chunxiang, L. Hongpeng and L. Licheng, *China Synthetic Fiber Industry*, 2009, **2**, 7-10.
29. C. R. Bohn, J. R. Schaefgen and W. O. Statton, *Journal of Polymer Science*, 1961, **55**, 531-549.
30. Z. Bashir and S. Rastogi, *Journal of Macromolecular Science. Part B : Physics*, 2005, **44**, 55 - 78.
31. K. I. Suresh, K. S. Thomas, B. S. Rao and C. P. R. Nair, *Polym. Adv. Technol.*, 2008, **19**, 831-837.
32. S. Okajima, M. Ikeda and A. Takeuchi, *Journal of Polymer Science Part a-1-Polymer Chemistry*, 1968, **6**, 1925-1933.
33. J. Zhang, Y. Zhang, D. Zhang and J. Zhao, *J. Appl. Polym. Sci.*, 2012, **125**, E58-E66.
34. L. G. Wallner and K. Riggert, *Journal of Polymer Science Part B-Polymer Letters*, 1963, **1**, 111-114.
35. M.-S. Khil, S. R. Bhattarai, H.-Y. Kim, S.-Z. Kim and K.-H. Lee, *Journal of Biomedical Materials Research Part B: Applied Biomaterials*, 2005, **72B**, 117-124.
36. E. Smit, U. Buttner and R. D. Sanderson, *Polymer*, 2005, **46**, 2419-2423.
37. W. E. Teo, R. Gopal, R. Ramaseshan, K. Fujihara and S. Ramakrishna, *Polymer*, 2007, **48**, 3400-3405.
38. M. Yousefzadeh, M. Latifi, W.-E. Teo, M. Amani-Tehran and S. Ramakrishna, *Polym. Eng. Sci.*, 2011, **51**, 323-329.
39. F. Dabirian, Y. Hosseini and S. A. H. Ravandi, *The Journal of The Textile Institute*, 2007, **98**, 237-241.
40. F. Dabirian and S. A. H. Ravandi, *Fibres & Textiles in Eastern Europe*, 2009, **17**, 45-47.
41. F. Hajiani, A. A. Jeddi and A. A. Gharehaghaji, *Fibers and Polymers*, 2012, **13**, 244-252.
42. A. M. Afifi, S. Nakano, H. Yamane and Y. Kimura, *Macromol. Mater. Eng.*, 2010, **295**, 660-665.
43. U. Ali, Y. Zhou, X. Wang and T. Lin, *Journal of The Textile Institute*, 2012, **103**, 80-88.
44. S. F. Fennessey and R. J. Farris, *Polymer*, 2004, **45**, 4217-4225.
45. E. V. Thompson, *Journal of Polymer Science Part B: Polymer Letters*, 1966, **4**, 361-366.
46. B. Cassel and B. Twombly, *American Society for Testing and Materials*, 1991, **STP1136**, 12.
47. Z. Bashir, A. R. Tipping and S. P. Church, *Polym. Int.*, 1994, **33**, 9-17.
48. B. Jasse and J. L. Koenig, *Journal of Macromolecular Science, Part C*, 1979, **17**, 61-135.
49. R. Zbinden, *Infrared spectroscopy of high polymers*, Academic Press, New York, 1964.